PNAS
www.pnas.org

Supplementary Information for

Helical nanofibers yarn enabling highly-stretchable engineered micro-tissue

Yiwei Li,[1#] Fengyun Guo,[2,3#] Yukun Hao,[1] Satish Kumar Gupta,[1] Jiliang Hu,[1] Yaqiong Wang,[2] N ü Wang,[2] Yong Zhao,[2*] Ming Guo[1*]

*To Ming Guo and Yong Zhao correspondence may be addressed
Email: guom@mit.edu; zhaoyong@buaa.edu.cn

This PDF file includes:

Supplementary text
Figs. S1 to S5

www.pnas.org/cgi/doi/10.1073/pnas.1821617116

Materials and Methods

Electrospinning of nanofibers. The electrospinning process was performed using a home-made setup including a high voltage power supply, a syringe with stainless steel blunt-ended needle and a rotating mandrel collector. 1 mL homogeneous precursor solution was added to a 2 mL syringe. The working distance between the needle tip and collector was set as 15 cm. By adjusting the voltage and controlling the time, we obtained the fibrous membrane.

Fabrication of helix scaffolds. We cut the fibrous membrane into rectangular strips of dimension 2 cm x 25 cm. First, the strip was suspended horizontally with two ends fixed on an electric motor and a metal block, respectively. Then the strip was twisted into a straight yarn at a speed of 120 turns/min. After that, the straight yarn was spun into a hierarchical helix yarn by continued over-twisting. Finally, the yarn was detached from the motor and it maintained a stable hierarchical helix configuration.

Mathematical Modeling of the helix strand. According to the experimentally examined samples, the simulated geometry is generated as an ideal helix with 4.5 coils (Figure 3A). The geometry of the hierarchical helix strand is described by a set of parametric equations:

$$x = R\cos\alpha s - r\cos\gamma s\cos\alpha s + \beta r\sin\gamma s\sin\alpha s;$$

$$y = R\sin\alpha s - r\cos\gamma s\sin\alpha s + \beta r\sin\gamma s\cos\alpha s;$$

$$z = \beta \mathrm{s} + \alpha \mathrm{R}\, r\sin\gamma s.$$

The simulation parameters chosen are R=10, r=5, β=0.174, α=0.1, γ=1, $s \in [0,300]$ which yield the initial length of the scaffold as ~60. The hierarchical helix scaffold comprises of 4.5 hierarchical helix strands and separated by 1000 beam units. The section radius of the beam unit is 0.5.

Cell culture. Mouse embryonic fibroblasts (MEFs) and MDA-MB-231 cells were cultured using DMEM medium supplemented with 10% Fetal Bovine Serum (FBS). Clonally derived mouse MSCs (OP9) purchased from American Type Cell Culture (ATCC) were expanded sub-confluently in high-glucose, 10 fetal bovine serum-supplemented with Dulbecco's Modified Eagle media (complete DMEM).

Cell viability assay. To test the biocompatibility of helix scaffold made from various types of materials, cells on the fiber were incubated in DMEM cell culture medium. LIVE/DEAD cell assay was carried out after 1 day, 2 days, 3 days, 4 days and 5 days.

Immunostaining. Cells were then fixed with 4% paraformaldehyde for 30 min at room temperature. Cells on coverslips were penetrated by 0.2% tritton-X100 for 1 hour and incubated with primary antibodies overnight. After careful removal of primary antibodies by rinsing with PBS, cells were treated with secondary antibodies for 4 hours at room temperature. Following extensive washing, stained cells were imaged with confocal microscopy (Leica SP8).

Cell proliferation by Ki67 staining. Cells cultured on helix scaffold or 2D substrate were fixed with 4% paraformaldehyde for 20 min at room temperature. Then, cells were permeabilized with 0.2% Triton X-100 in PBS for 1 hour and blocked with 3% BSA in PBS containing 0.01% Triton X-100 for 3 hours. Cells were rinsed and stained with

rabbit anti-Ki67 antibody (Cat#9129, Invitrogen) for 2 hours. After rinsing with PBS for at least 3 hours, colonies were incubated overnight at 4 ℃ with secondary antibody Alexa 568 goat-anti-rabbit (A11036, Invitrogen) in block solution. Following removal of residual antibodies, stained ISCs and organoids were imaged with confocal microscopy (Leica SP8).

3D volume measurement. 3D stained cell images were obtained using 63x/1.2NA water immersion lens on a confocal microscope (Leica SP8, Germany). Cells that we imaged were randomly picked. The optical cross-sections were recorded at 0.15 micron z-axis intervals to show intracellular, nuclear, and cortical fluorescence. x-y pixel size was chosen to be comparable to z-axis interval to achieve better voxel resolution and better deconvolution results. The 3D image was deconvolved using a Huygens Software before 3D visualization. 3D visualization was carried out using ImageJ, AMIRA software and LAS X 3D Visualization from Leica. The volume of cells and cell nuclei were calculated by counting voxel number, after thresholding the stack using a home-built MATLAB algorithm. The confocal measurement of cell volume has been previously compared with measurement using atomic force microscopy (AFM) and super resolution structured illustration microscopy, showing consistent results for both the cell height and cell volume(25).

Myogenic differentiation. To induce myogenesis, MSCs on fibers or substrates were cultured with myogenic medium for more than 10 days: complete DMEM supplemented with 5% horse serum, 0.1 μM dexamethasone, and 50 μM hydrocortisone, cycling every two days. To assess myogenesis efficiency, immunofluorescent staining of the myogenic differentiation marker (MHC) was performed. Cells were rinsed twice with PBS, fixed for 20 min with 4% paraformaldehyde and then washed three times with PBS. The cells were incubated with 3% hydrogen peroxide in PBS for 10 min to quench endogenous peroxidase enzyme activity and nonspecific sites were blocked by incubation in blocking buffer (PBS, 10% HS, 0.1% Triton X-100) for an additional 60 min. The cells were washed three times after blocking for 5 min and incubated for 1 hour in blocking buffer containing anti-MHC. The cells were rinsed extensively in blocking buffer and stained with secondary antibody Goat anti-Rabbit Alexa 488 according to manufacturer's manual.

Statistical analysis and sample information. Statistically significant differences between the means of two groups were assessed using a Student's t-test, whereas data containing more than two experimental groups were analyzed with a one-way analysis of variance followed by a Bonferroni's multiple comparison test. All statistical analyses were performed in the Origin 9.0 software. *$p<0.05$, **$p<0.01$, ***$p<0.001$, respectively.

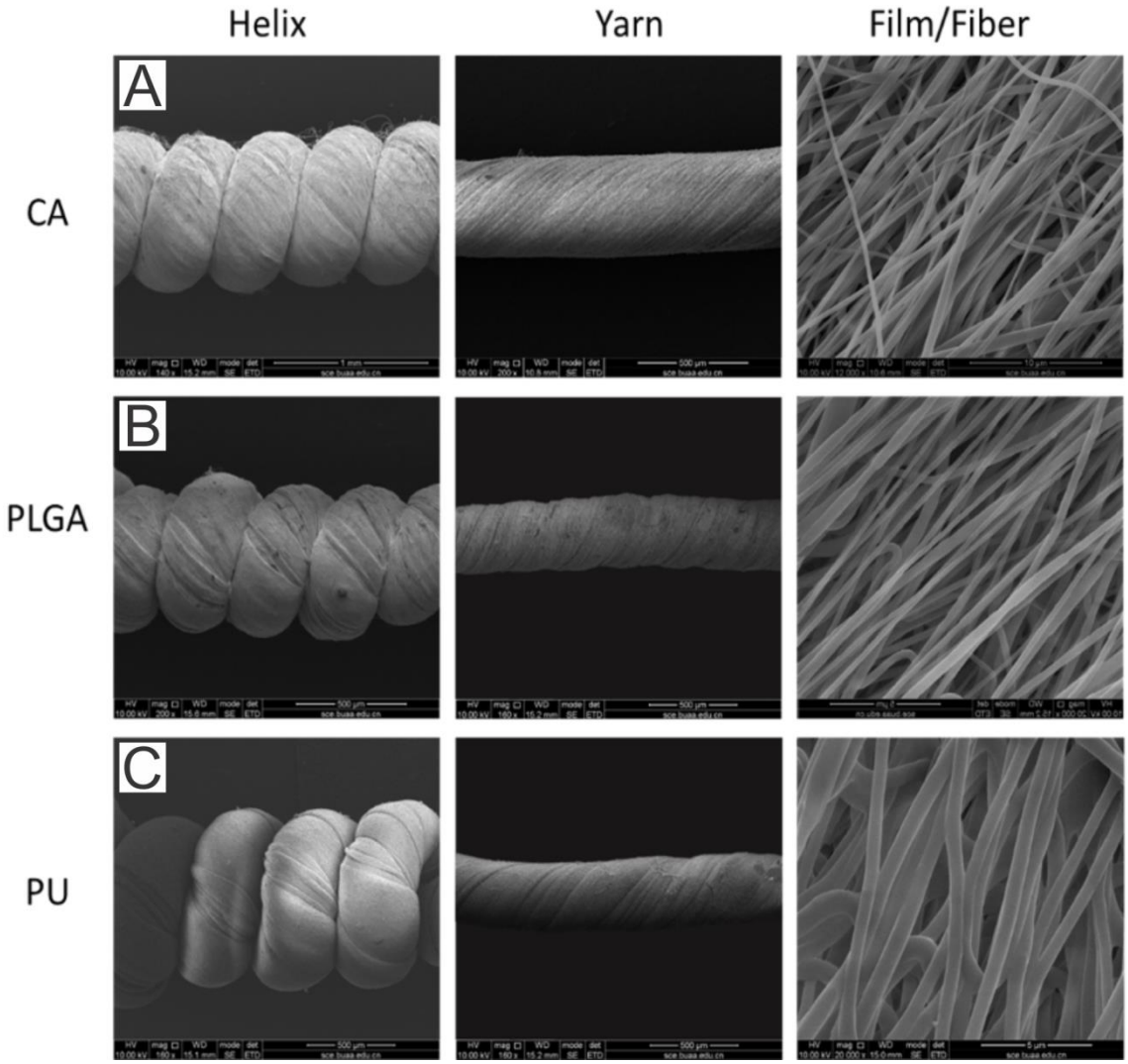

Fig. S1. SEM images show the hierarchical helical nanofibers yarns fabricated by various building blocks. CA, cellulose acetate; PLGA, poly(lactic-co-glycolic acid); PU, polyurethane.

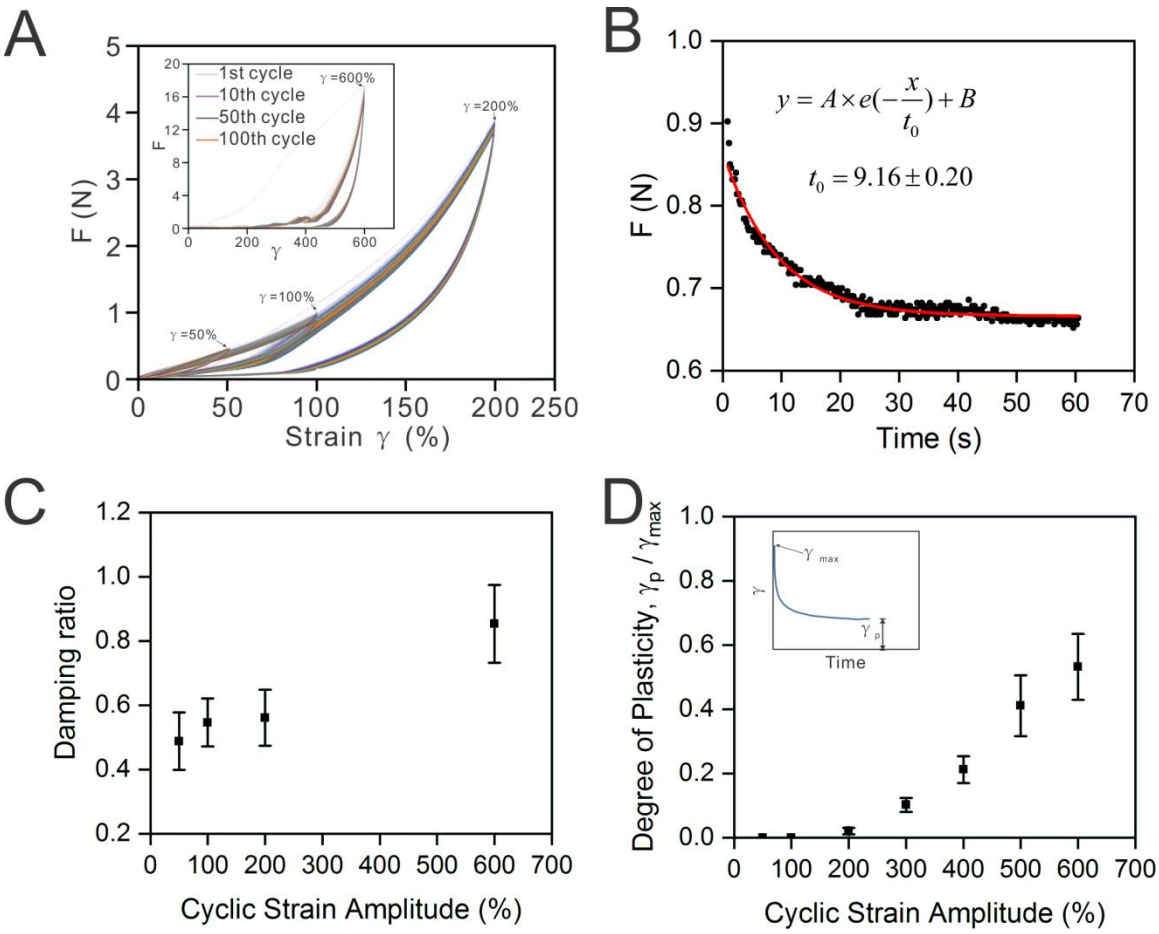

Fig. S2. Characterization of viscoelasticity and plasticity of helical nanofibers yarn. (A) Force-strain curves of cyclic loading on helical nanofibers yarn at different strain amplitudes at a constant strain rate of 10 mm per minute. (B) A representative force relaxation curve of a helical nanofibers yarn. A helical fiber is strained to 100% strain at a high speed, and maintained at this strain while force is recorded over time. The force relaxation curve is fitted to an exponential function to obtain a characteristic relaxation time. (C) Analysis of damping capacity of helical nanofibers yarn under different cyclic strain amplitudes. (D) Analysis of the degree of plasticity under different strains. The degree of plasticity here is computed as the ratio of the residual strain after recovery to the maximum strain applied, as indicated in the inset.

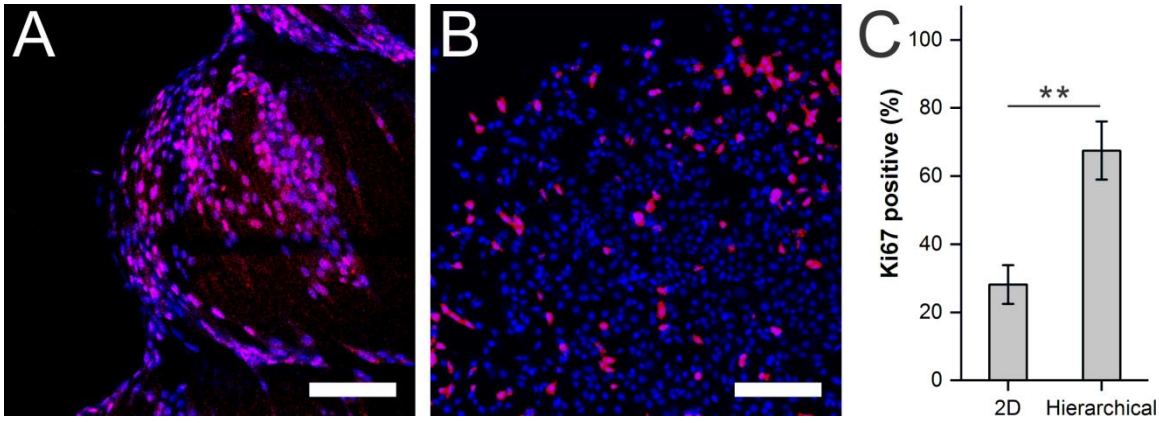

Fig. S3. The hierarchical helix scaffold promotes cell proliferation as indicated by Ki67 staining. Ki67 staining of cells growing on helix scaffold (A) as compared to cells on 2D substrate (B), showing an elevated cell proliferation ratio (C).

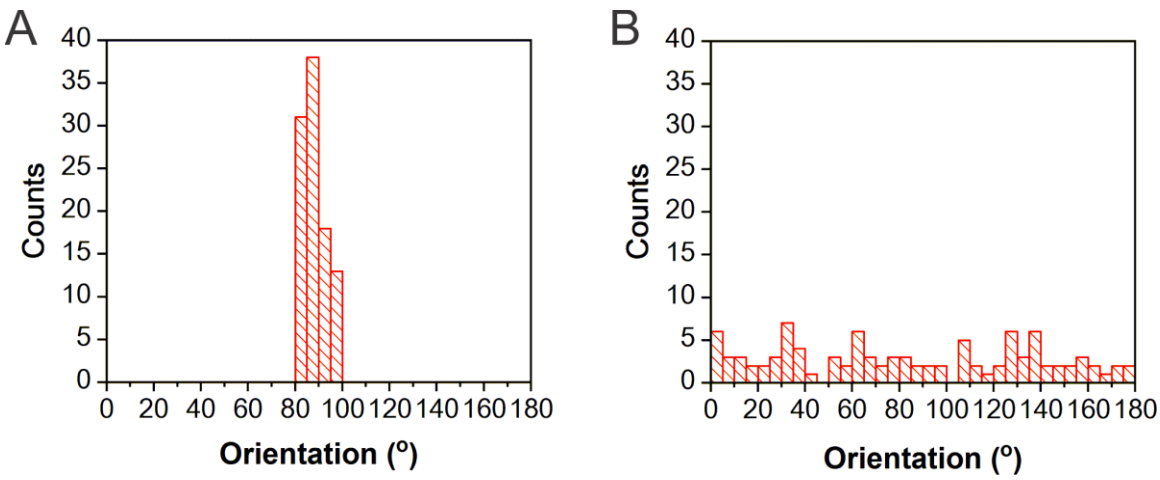

Fig. S4. The orientation of single cells cultured on helix scaffold (A) and 2D substrate (B), shows that the cells growing on helical nanofibers yarn are aligned while cells on 2D substrates are randomly orientated.

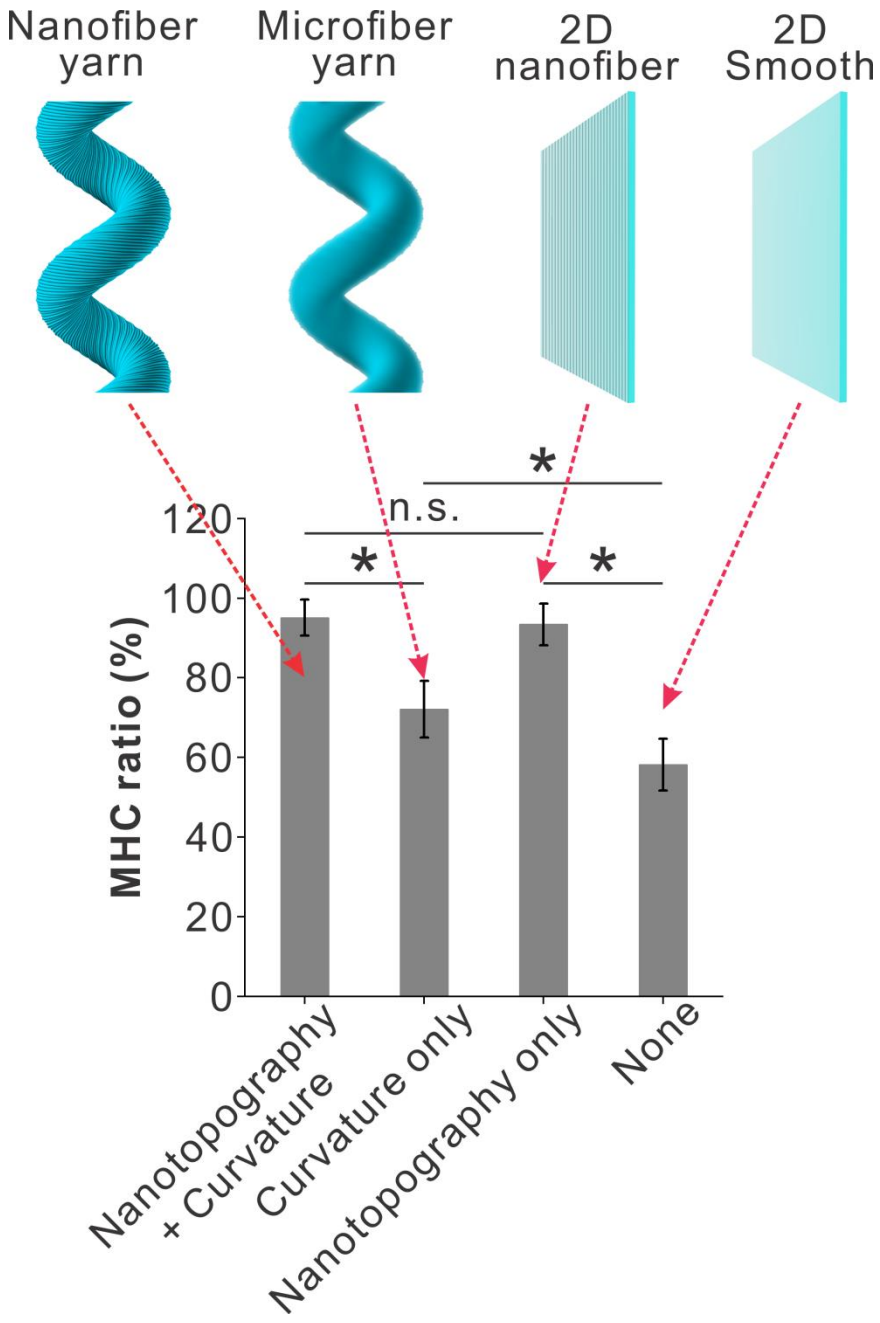

Fig. S5. Comparison of the effects of nanotopography and curvature on myogenic differentiation of MSCs. The results show that the aligned nanotopographic feature generates sufficient enhancement effect on myogenic differentiation. As comparison, the microscale curvature also generates elevated myogenesis, but weaker than the effect from aligned nanostructures.